

Rapid Growth of Galactic Supermassive Black Holes through Accreting Giant Molecular Clouds during Major Mergers of their Host Galaxies

CHI-HONG LIN ¹, KE-JUNG CHEN ¹ AND CHORNG-YUAN HWANG ²

¹*Institute of Astronomy and Astrophysics, Academia Sinica, Taipei 10617, Taiwan R.O.C.*

²*Institute of Astronomy, National Central University, Taoyuan 32001, Taiwan R.O.C.*

ABSTRACT

Understanding the formation of the supermassive black holes (SMBHs) present in the centers of galaxies is a crucial topic in modern astrophysics. Observations have detected the SMBHs with mass M of $10^9 M_\odot$ in the high-redshift galaxies with $z \sim 7$. However, how SMBHs grew to such huge masses within the first billion years after the big bang remains elusive. One possible explanation is that SMBHs grow quickly through the frequent mergers of galaxies, which provides sustainable gas to maintain rapid growth. This study presents the hydrodynamics simulations of the SMBHs' growth with their host galaxies using the GIZMO code. In contrast to previous simulations, we have developed a giant molecular cloud (GMC) model by separating molecular-gas particles from the atomic-gas particles and then evolving them independently. During major mergers, we show that the more massive molecular gas particles cloud bear stronger dynamical friction. Consequently, GMCs are substantially accreted onto the galactic centers that grow SMBHs from $\sim 10^7 M_\odot$ to $\sim 10^9 M_\odot$ within 300 Myr, explaining the rapid growth of SMBHs, and this accretion also triggers a violent starburst at the galactic center. Furthermore, we examine the impact of minor mergers on the bulge of a Milky-Way-like galaxy and find that the size and mass of the bulge can increase from 0.92 kpc to 1.9 kpc and from $4.7 \times 10^{10} M_\odot$ to $7 \times 10^{10} M_\odot$.

Keywords: Supermassive black holes, Galaxy evolution, Galactic bulge, Starburst galaxies, Galaxy mergers, Computational astronomy.

1. INTRODUCTION

Supermassive black holes (SMBHs) have been discovered in most galaxies (e.g., Lynden-Bell 1969; Kormendy & Richstone 1995; Magorrian et al. 1998), suggesting that the existence of SMBHs may be associated with their host galaxies. Growing evidence shows that the mass of an SMBH is correlated to its galactic bulge, including luminosity (e.g., Kormendy & Richstone 1995; Wu & Han 2001; Graham & Driver 2007; Marconi & Hunt 2003), stellar mass (e.g., McLure & Dunlop 2002; Häring & Rix 2004; Graham et al. 2001), size (Ferrarese 2002; Lauer et al. 2007), and dynamics and velocity dispersion σ (e.g., Ferrarese & Merritt 2000; Tremaine et al. 2002; Aller & Richstone 2007; Soker & Meiron 2011; King & Pounds 2015). These observational results exhibit strong connections between the SMBHs and their host galaxies (e.g., Wandel 2002; Feoli et al. 2011; Kormendy & Ho 2013).

The SMBH of the Milky Way (MW), known as “Sagittarius A*”, has a mass of $(4.1 \pm 0.6) \times 10^6 M_\odot$ (Ghez et al.

2008). The maximum accretion rate of the Sagittarius A* is $8 \times 10^{-5} M_\odot \text{ yr}^{-1}$, which has been determined from X-ray and infrared research (Quataert et al. 1999). However, Mortlock et al. (2011) and Venemans et al. (2015) discovered SMBHs of $10^9 M_\odot$ in the early universe at $z > 6.5$. To grow an SMBH with a mass of one thousand times larger than that of Sagittarius A*, high accretion rates are required in a very short period (The universe's age is only $\simeq 0.83$ Gyr at $z = 6.5$). How an SMBH grows in a short time and how the host galaxy provides a suitable environment for the growth remain unknown. One possible explanation is that an SMBH grows through galaxy mergers (Volonteri & Rees 2005), which supply the SMBH with a new gas reservoir. In a fully developed isolated disk galaxy, the dark matter, gas cloud, and stars have reached the state of relaxation; the galaxy is in quasi-dynamical equilibrium. Therefore, most of the gas and stars move along their stable orbits without migrating toward the galactic center. In contrast, during a major merger between two galaxies, the tidal forces from their interaction can induce strong,

non-axisymmetric perturbations that disrupt the equilibrium of both galaxies and alter the motion of stars and gas. As a result, some stars and gas may be shifted towards the galaxy’s center, forming a rich reservoir of gas that can fuel the growth of an SMBH during the phase of a galaxy merger. For example, an SMBH can rapidly grow during a wet merger (Hopkins et al. 2006) through a super-Eddington accretion (Takeo et al. 2019). However, how to maintain an enduring super-Eddington accretion remains unclear. Simultaneously, the feedback of SMBHs also self-regulates its accretion and star formation rates inside the galactic bulge (Springel et al. 2005a). Simulations of galaxy merger by Di Matteo et al. (2005) showed that an SMBH could grow from $4 \times 10^5 M_\odot$ to $10^8 M_\odot$ in 1.5 Gyr, but growing an SMBH to $\sim 10^9 M_\odot$ within 1 Gyr is still challenging.

If the gas accretion powers the rapid growth of a galactic SMBH during major mergers of their host galaxies, such a substantial influx of gas should also drive a violent star formation activity at the galactic center. This so-called nucleus starburst of a star formation rate (SFR) $\sim 100 - 1000$ higher than normal galaxies have been observed in interacting galaxies (e.g., Joseph & Wright 1985, Schweizer 2005). Since stars form from molecular gas, we suspect that GMCs can also be used to grow an SMBH. GMCs contain dense molecular gas and have a more compact structure than diffuse gas. The difference in cloud masses between atomic gas clouds and GMCs leads to distinct dynamical friction effects from the surrounding medium in their host galaxy. Compact and massive GMCs are subject to stronger dynamical friction force from the background medium, consisting of gas, stars, and dark matter. This mechanism causes GMCs to migrate efficiently toward the galactic center during galaxy mergers. Therefore, we propose that GMC accretion can be a viable channel to facilitate rapid SMBH growth and generate a nucleus starburst in major mergers.

Due to the strong impact of a galaxy-galaxy collision, the original spiral structures of galaxies can be disrupted during major mergers. On the other hand, minor mergers are more promising for growing a galaxy’s size (Bédorf & Portegies Zwart 2013) and contributing to a bulge’s mass (Hopkins et al. 2010), producing irregular galaxies (Bournaud et al. 2005). Furthermore, a minor merger may account for the inner components (inner discs and rings) in unbarred spiral galaxies (Eliche-Moral et al. 2011).

Therefore, we examine the possibility of SMBHs’ rapid growth via accreting molecular gas in major and minor galaxy mergers using high-resolution galaxy simulations with the GIZMO code. The structure of this paper is

as follows. Sec. 2 describes the simulation setup and the relevant physics required to model galaxy mergers. Then, the growth of SMBHs and the associate SF activities during galaxy mergers are presented in Sec. 3. Finally, we discuss and compare the results with previous studies in Sec. 4 and conclude in Sec. 5.

2. NUMERICAL METHODS

2.1. The GIZMO code

We perform our galaxy simulations using the mesh-free hydrodynamic code: GIZMO (Hopkins 2015). It is an open-source code that is based on the widely used cosmological code, GADGET-2 (Springel 2005), for the domain decomposition and N-body algorithms. We employ the Meshless Finite-Mass (MFM) and Meshless Finite-Volume (MFV) methods in our GIZMO simulations. In the MFM and MFV methods, each particle is treated as a mesh-generating point that defines the volume. The physical quantities of each particle determine the fluid properties. The code solves the hydrodynamics equations by integrating the domain of each particle. Compared to other public codes in astrophysical simulations, GIZMO (Hopkins 2015) exhibits superior performance in conserving angular momentum, which is critical for modeling the dynamics of galaxy mergers.

2.2. Simulation setup

We create pre-merging galaxies using the MW as a reference and divide them into gas-poor and gas-rich galaxies. The gas-poor galaxies, with a mass of $\sim 1.46 \times 10^{12} M_\odot$, are modeled based on parameters obtain from Gaia observations (Brown et al. 2016; Li 2016; Posti & Helmi 2019) and the N-body study by Fujii et al. (2019). On the other hand, the gas-rich galaxies adopt the same parameters as the MW but with an artificially increased gas mass of $1.42 \times 10^{11} M_\odot$. The population of gas-rich galaxies likely dominates among high-redshift galaxies of $z > 2$ (Solomon & Vanden Bout 2005).

Herein, both the gas-poor and gas-rich galaxies here are called $10^{12} M_\odot$ disk galaxies. In addition to these galaxies, we generate dwarf galaxies with mass $\sim 1 \times 10^{11} M_\odot$ for minor mergers. The detailed parameters of these three types of galaxies are listed in Table 1. Then, we use the DICE code (Perret et al. 2014) with input parameters from Table 1 and create the initial galaxies for evolution in the GIZMO code. The simulation considers the following scenarios:

1. Model M_{poor} denotes a major merger of two gas-poor galaxies.

Table 1. Table of the initial conditions.

Component	Physical Parameters	G_{rich}	G_{poor}	G_{dwarf}
Whole Galaxy	M_{200} [$10^{10} M_{\odot}$]	146	146	10
	V_{200} [$\text{km} \cdot \text{s}^{-1}$]	166.1	166.1	–
	Halo spin parameter (λ)	0.04	0.04	0.04
Gas	Mass of atomic gas [M_{\odot}]	6.2×10^{10}	1.5×10^{10}	1.5×10^9
	Mass of molecular gas [M_{\odot}]	8×10^{10}	6×10^9	2×10^8
	radial cut [kpc]	15	15	10
	Mass of an atomic particle [M_{\odot}]	2×10^4	5×10^3	5×10^3
	Mass of a molecular particle [M_{\odot}]	10^6	10^6	10^6
	Distribution forms		Exponential disk+sech-z	
	Mean metallicity of the particles [Z_{\odot}]		2×10^{-6}	
Gravitational softening lengths [kpc]		0.001		
Dark Matter	Mass [M_{\odot}]	1.2×10^{12}	1.2×10^{12}	9.5×10^{10}
	radial cut [kpc]	300	300	100
	Concentration parameter	13	13	4.4
	Mass of a DM particle [M_{\odot}]	5×10^6	5×10^6	5×10^6
	Distribution		NFW profile	
Gravitational softening lengths [kpc]		0.05		
Stellar Disk	Mass [M_{\odot}]	1.1×10^{11}	2.3×10^{11}	2.3×10^9
	radial cut [kpc]	20	20	10
	Mass of a star particle [M_{\odot}]	10^6	10^6	10^6
	Distribution		Exponential disk+exponential-z	
	Mean metallicity of the particles [Z_{\odot}]		0.01	
Gravitational softening lengths [kpc]		0.02		
Stellar Bulge	Mass [M_{\odot}]	8×10^9	1.7×10^{10}	1×10^9
	radial cut [kpc]	2	2	0.5
	Mass of a star particle [M_{\odot}]	10^6	10^6	10^6
	Distribution		Einasto profile	
	Mean metallicity of the particles [Z_{\odot}]		0.001	
Gravitational softening lengths [kpc]		0.02		

NOTE—The initial mass of an SMBH seed in each galaxy model is not an input parameter. Instead, this seed mass is simulated based on the recipe discussed in Sec. 2.4.

2. Model M_{rich} denotes a major merger of two gas-rich galaxies.
3. Model M_{dwarf} denotes a minor merger of one gas-poor galaxy with two dwarf galaxies.

For the major mergers, we place two galaxies in a $(100 \text{ kpc})^3$ cubic simulation box, and their separation is 30 kpc with an approaching velocity of 180 km s^{-1} . The two galaxies will collide in 0.1 billion years after the simulation begins. For the minor merger case, we place a gas-poor galaxy and two dwarf galaxies in the simulation box. The gas-poor galaxy is located at the center of the box, while two dwarf galaxies are separately placed 37

kpc and 55 kpc away from it. The two dwarf galaxies approach the gas-poor galaxy with a velocity of 120 km s^{-1} . The initial conditions for these three scenarios are illustrated in Table 2.

We plan to initially evolve three models for five billion years (5 Gyr). As the simulations evolve, their time step shrinks rapidly at the late time due to the complicated interplay between the gas flow and SMBH/SNe feedback. It makes the simulation very computationally expensive and forces us to stop evolving the major merger simulations at $t \sim 2 \text{ Gyr}$ and $t \sim 3.5 \text{ Gyr}$ for the minor merger case. The simulation results are analyzed with python packages SciPy (Virtanen et al.

2020), `pylab` (Hunter 2007), and `h5py` (Collette 2013) with data visualization using `Matplotlib` (Hunter 2007) and the `SPLASH` code (Price 2007).

Table 2. Table of the galaxy merger parameters.

Name	d_{ini} [kpc]	v_i [km · s ⁻¹]	s [deg]	i [deg]
$M_{\text{poor}}, M_{\text{rich}}$	30	180	0	-90
M_{dwarf}	37	120	45	45
	55	120	0	90

NOTE— d_{ini} is the initial separation, v_i is the initial velocity, s is the spin angle, and i is the inclination angle.

2.3. ISM Physics in GIZMO

In reality, the interstellar medium (ISM) structure is incredibly complex, with different phases of gas, dust, and other baryonic components. Modeling the cold and dense regions is challenging because of the extremely small timesteps required for hydrodynamic simulations (Marinacci et al. 2019). To overcome this challenge, a common solution is to use an “effective equation of state (eEOS)” (Springel & Hernquist 2003; Vogelsberger et al. 2013) that treats the multi-phase ISM gas as an entity and calculates its EOS based on the contribution from each phase of the ISM. Therefore, we use a widely-used two-phase sub-grid model based on McKee & Ostriker (1977); Springel & Hernquist (2003) added molecular gas particles to model the galactic ISM. This model includes the hot atomic gas ($T = 3 \times 10^8$ K) for the SN ejecta, cold atomic gas ($T = 10^3$ K) for the diffuse ISM, and cool molecular gas ($T = 30$ K) for the GMCs. The cooling and heating of the two-phase atomic gas are modeled through ionization and recombination of hydrogen/helium, photo-electrons, collisional excitations, bremsstrahlung, cosmic rays, and Compton scattering for temperatures above 10^4 K (Hopkins et al. 2018; Faucher-Giguère 2020). For the metal cooling, GIZMO uses a cooling table of 11 elements (H, He, C, N, O, Ne, Mg, Si, S, Ca, and Fe) calculated by CLOUDY (Ferland et al. 1998; Wiersma et al. 2009). For molecular gas cooling, additional fine-structure and molecular cooling functions from Robertson & Kravtsov (2008) extend the cooling curves down to ~ 10 K (Hopkins et al. 2018).

The gas in GIZMO comprises atomic and molecular gas particles. We set the mass ratio between molecular and

atomic gas, $M_{\text{H}_2}/M_{\text{HI}} \sim 1.3$ for the gas-rich merger based on the semi-analytic models (Popping et al. 2014), and ~ 0.4 for the gas-poor merger based on the observation of our Milky Way (Brown et al. 2016; Li 2016; Posti & Helmi 2019). Because the simulation did not consider the exchange processes between atomic and molecular gas, an atomic gas particle never turns into a molecular particle, and vice versa.

ISM Observations (Solomon et al. 1979; Solomon & Sanders 1980) suggested that most galactic molecular gas resides in GMCs. For simplicity, we assume all molecular gas in the simulation belongs to massive GMC particles, and each particle mass is set to $\sim 10^6 M_{\odot}$ based on GMC observations (Cohen et al. 1985; Solomon et al. 1987). Meanwhile, each atomic gas particle has a mass of $\sim 10^3 - 10^4 M_{\odot}$, which is ~ 100 times less than a molecular gas particle. The mass difference between atomic and molecular gas particles can alter their kinetics through dynamical friction. This force arises when an object moves through the galaxy and experiences a drag force due to the gravitational pull from gas, stars, and dark matter in the background. In sum, the dynamical friction can differentiate the dynamics of atomic gas and GMCs during major mergers. Section 4.1 will delve into how this process takes place. The galactic star formation in the simulation follows the star formation model of Springel & Hernquist (2003), which only allows stars to form from molecular gas particles. The gas particles with a density $> 100 \text{ cm}^{-3}$ and satisfy other star formation criteria (e.g., the Jeans criterion); these gas particles are then converted into star particles with a star formation efficiency (SFE) based on the free-fall time of a gas particle divided by the SF timescale of 40 Myr used in the code. We use the stellar feedback recipe from the AGORA project (Kim et al. 2016), which applies “pure thermal energy dump” feedback: mass, metals, and thermal energy injected locally in a simple kernel-weighted fashion around the star particles.

Once the star particles form from molecular gas, they immediately produce strong stellar feedback. Besides the thermal feedback, the algorithm assumes the newly forming star particles to have an IMF-averaged number of core-collapse SNe, which all explode at once when the age of a star particle turns into 5 Myr old and assumes each core-collapse SN releases 10^{51} erg explosion energy and 14.8 M_{\odot} ejecta containing 2.6 M_{\odot} of metals with a solar abundance.

2.4. Modeling the physics of SMBHs

Similar to previous studies, we use a sub-grid prescription (Hopkins & Quataert 2011) to address the physical processes in an SMBH. We permit BH seeds (Hoyle &

Fowler 1962; Rees 1984; Chen et al. 2014; Woods et al. 2019) to be formed in the galaxy’s central region and allow them to merge to form an SMBH seed which accretes mass using the sub-grid accretion model from Hopkins & Quataert (2010). These BH seeds are thought to originate from the collapse of supermassive stars of mass $\approx 10^4 - 10^6 M_\odot$ formed in the atomic cooling halos of mass $\sim 10^9 M_\odot$ at $z \sim 10 - 15$ (Begelman 2010; Inayoshi et al. 2020; Das et al. 2021). The low-metallicity and high-dense environment are required to form these supermassive stars. Therefore, the criteria of BH seed formation are similar to the massive star formation in galaxy simulation. Based on Lamberts et al. (2016) and Grudić et al. (2018), the formation probability of BH seeds can be expressed as

$$\frac{dP_{\text{seed}}}{dM_*} = \frac{1}{M_n} [1 - \exp(-\Sigma)] \exp\left(\frac{-Z}{0.01 Z_\odot}\right), \quad (1)$$

where M_* is the stellar mass, M_n is a normalization parameter, Z is the gas metallicity, and Σ is the surface density in units of 1 g cm^{-2} .

Equation (1) can be physically interpreted as indicating that BH seed particles tend to form in regions characterized by high surface density $\gg 1 \text{ g cm}^{-2}$ and low metallicity $\ll 0.01 Z_\odot$. Under these conditions, there is a high likelihood that a given gas particle will become a BH seed with a mass of $\sim 10^6 M_\odot$. As listed in Table 1, the initial gas metallicity in both G_{rich} and G_{poor} is $2 \times 10^{-6} Z_\odot$, which soon will be increased by SN metals from deaths of massive stars within a few million years after the galaxies start to evolve. Therefore, the initial BH seeds only form at the innermost region ($< 0.3 \text{ kpc}$) at the beginning of the simulations due to the high-density and low-metallicity environment. These BH seeds then move toward the galactic center and eventually merge into a more massive seed, which we refer to as the SMBH seed.

The actual size of the accretion disk around the SMBH is estimated to be $2 - 10 \text{ pc}$. Unfortunately, our simulation can only achieve the highest resolution of $\sim 20 \text{ pc}$, so we cannot resolve the structure of the accretion disk. If a gas or star particle is located within 20 pc around the SMBH, then the code check criteria: (1). Is the particle gravitationally bound to the SMBH? (2). Is the apo-centric radius of the particle about the SMBH also $< 20 \text{ pc}$? If both are true, the particle is immediately “captured” by the SMBH.

The physical properties of the accretion disk around an SMBH can be understood using the standard α disk model from (Shakura & Sunyaev 1973). However, the detailed process of mass transfer from the disk to the SMBH can only be understood through GRMHD sim-

ulations, which is far beyond the scope of this study. Therefore, we assume a steady-state accretion disk and allow $\dot{M}_{\text{BH}} = \dot{M}_{\text{disk}}$.

An accreting SMBH grows in mass and posits strong feedback to its surroundings. The intrinsic bolometric luminosity is $L_{\text{bol}} \equiv \epsilon \dot{M}_{\text{BH}} c^2$, where $\epsilon \sim 0.1$ is the radiative efficiency. This energy injection is equally distributed on the thermal energy of gas particles swirling around the SMBH (Springel et al. 2005b). The injected energy immediately increases the temperatures and pressures of the associated gas particles that drive a strong outflow and impact the entire galaxy. Besides this thermal energy injection, we also consider the mechanical feedback from an SMBH by including an accretion disk wind model (Hopkins et al. 2016). The time-dependent mass and momentum from the wind are calculated with a mass loading factor of $\beta \equiv \dot{M}_{\text{wind}}/\dot{M}_{\text{BH}} = 0.5$ and wind velocity $v_{\text{wind}} = 30000 \text{ km s}^{-1}$ based on observation (Moe et al. 2009; Borguet et al. 2012). Similar to thermal energy, the mass and momentum from the disk wind are injected into the gas particles swirling around the SMBH.

2.5. Defining the Bulge size

A galactic bulge contains a group of old stars in the center of a spiral galaxy. The bulge properties are highly related to its central SMBH (e.g., $M - \sigma$ relation in Ferrarese & Merritt (2000) and bulge mass relation in Häring & Rix 2004). The size and mass of a galactic bulge can be determined by fitting a profile of stellar density distribution with the sersic profile form (Sersic 1968):

$$I(R) = I_e \exp\left\{- (2n - 0.327) \left[\left(\frac{R}{R_e} \right)^{\frac{1}{n}} - 1 \right]\right\} + I_S \exp\left(-\frac{R}{R_S}\right), \quad (2)$$

where $I(R)$: the intensity at radius R , I_e : the effective intensity of the bulge, n : the sersic index, R_e : the effective radius of the bulge, I_S : the effective intensity of the disk, R_S : the effective radius of the disk.

During the galaxy merger, the bulge structure is poorly defined. Therefore, we adopt two methods to fit the bulge; if the stellar dynamics of the bulge are in equilibrium, we fit the bulge by assuming an SMBH in the bulge center. During a minor merger, the bulge stars take longer to reach equilibrium than during major mergers. Thus, we select the brightest region as the bulge center for fitting.

3. RESULTS

3.1. Rapid Growth of SMBH during the period of Major Mergers

First, we show the mass evolutionary tracks of SMBHs for the major merger of galaxies in the first Gyr in Figure 1. Overall, the average mass accretion rate is $\sim 5 M_{\odot} \text{ yr}^{-1}$ and $\sim 7 M_{\odot} \text{ yr}^{-1}$ for the M_{poor} and M_{rich} models, respectively. The mass accretion increased the mass of the SMBHs from $\sim 10^7 M_{\odot}$ to $10^9 M_{\odot}$ within 300 Myr. In the simulation, the Eddington limit is used to cap the maximum SMBH accretion rate, so the super-Eddington accretion cannot occur through the gas accretion. However, we find an extremely rapid growth of SMBH in the first 10 Myr in Figure 1. Although this accretion rate behaves like a super-Eddington, it is actually driven by the merger of initial BH seeds instead of gas accretion. As mentioned in Sec. 2.4, multiple BH seeds can form in the inner region of ≤ 0.3 kpc at the beginning of the simulation. We find eight BH seeds formed in the M_{rich} run and three BH seeds formed in the M_{poor} run. After the BH seeds form, they move towards the galactic center and finally merge to form the SMBH seed within 10 Myr. The mass of the SMBH seed in the M_{poor} model is $5.6 \times 10^6 M_{\odot}$ and in the M_{rich} model is $4 \times 10^7 M_{\odot}$.

The evolution of the mass accretion rate of the SMBHs in Figure 1 shows oscillatory patterns which are likely driven by the SN or BH feedback. We estimate the energy injection rates from SNe and the SMBH to find the dominating feedback driving the oscillatory accretion rates. Based on Figure 1, the average accretion rate of SMBH is $\dot{m} \sim 5 M_{\odot} \text{ yr}^{-1}$, so the total thermal energy dumps to the SMBH surrounding area has the form $E_{\text{BH}} \simeq L_{\text{bol}} \simeq \epsilon \dot{m} c^2 \simeq 3 \times 10^{46} \text{ erg s}^{-1}$, assuming $\epsilon \simeq 0.1$. For the SNe feedback during starburst, we assume the typical explosion energy of an SN, 10^{51} erg . The energy injection is only $\sim 3 \times 10^{43} \text{ erg s}^{-1}$ for the SNe feedback by assuming the SFR in a starburst galaxy of $\sim 100 M_{\odot} \text{ yr}^{-1}$ with the Chabrier IMF (Chabrier 2003) and a galactic SNe rate of $\sim 0.01 \text{ yr}^{-1}$ (Rozwadowska et al. 2021). The SMBH feedback is $\sim 100 - 1000$ times stronger than the SN feedback. Therefore, the SMBH feedback is responsible for making the oscillatory patterns on the accretion rates of an SMBH.

The host galaxies' environment can affect the growth of the SMBH. For example, the SMBHs in gas-rich galaxy mergers can grow larger than those in gas-poor galaxy mergers. In Figure 3, we show the compositions of accretion history. We find that the molecular gas contributes to $> 95\%$ of the accreted mass and plays a major role in fueling the rapid growth of an SMBH. Mean-

while, stars and atomic gas only contribute to $< 5\%$ of mass accreted. The above result demonstrates that the critical ingredient of the rapid growth of SMBHs in the simulation is the accretion of molecular gas.

In comparison, we also perform another simulation identical to the gas-rich run but set the mass for the molecular and atomic gas both equal to $10^4 M_{\odot}$. As shown in Figure 4, this equal-mass model fails to demonstrate a rapid growth of SMBH. The average growth rate in equal-mass run is $\sim 10^{-3} M_{\odot} \text{ yr}^{-1}$, which is consistent with the values found in Di Matteo et al. (2005).

3.2. Starbursts

At the beginning of our galaxy simulation, star formation mainly occurs in the spiral arms and the bulge that hosts GMCs until the two galaxies collide. The SFR distribution of the major merger cases is shown in Figure 5. Many molecular-gas particles flow into the centers of two galaxies, triggering rapid star formation. In Figure 6, a high star formation rate is observed at the central region of $r \lesssim 1 \text{ kpc}$, contributing to over 50% of the star formation in the galaxy, and this high SFR lasts 150 Myr. In the simulation, we only allow star formation from molecular-gas particles; thus, the SFR distribution can reflect the importance of the dynamics of molecular gases. The starburst only occurs in the merger of gas-rich galaxies with a plentiful supply of molecular gas.

3.3. The bulge growth with minor merger

Since the bulge size for a detached galaxy is independent of the gas abundance, gas-poor and gas-rich galaxies have the same bulge size of 0.92 kpc. Moreover, the bulge sizes remain approximately constant during their evolution. A major merger cannot increase the bulge size of a spiral galaxy because this merger usually disrupts the original disk and bulge of galaxies. To investigate the growth of the bulge of a spiral galaxy, we consider minor mergers to avoid destroying the original structure of the primary galaxies. We consider the minor merger of a gas-poor galaxy with two dwarf galaxies with physical parameters from Table 1 and run this model for 3.5 Gyr. Figure 7 shows the evolution of bulge during the minor mergers. After two dwarf galaxies merge with the spiral galaxy, the bulge size increase by showing a larger bright central area in Figure 7. We then plot the evolution of bulge radius and mass in Figure 8 that shows the growths of bulge radius from 0.9 to ~ 1.9 kpc and bulge mass from $4.7 \times 10^{10} M_{\odot}$ to $7 \times 10^{10} M_{\odot}$ at the end of the simulation. The average growth rate of the bulge mass is $\sim 30 M_{\odot} \text{ yr}^{-1}$. The bulge of a disk galaxy can grow through minor mergers by swallowing the gas and dark matter of smaller galaxies. Therefore,

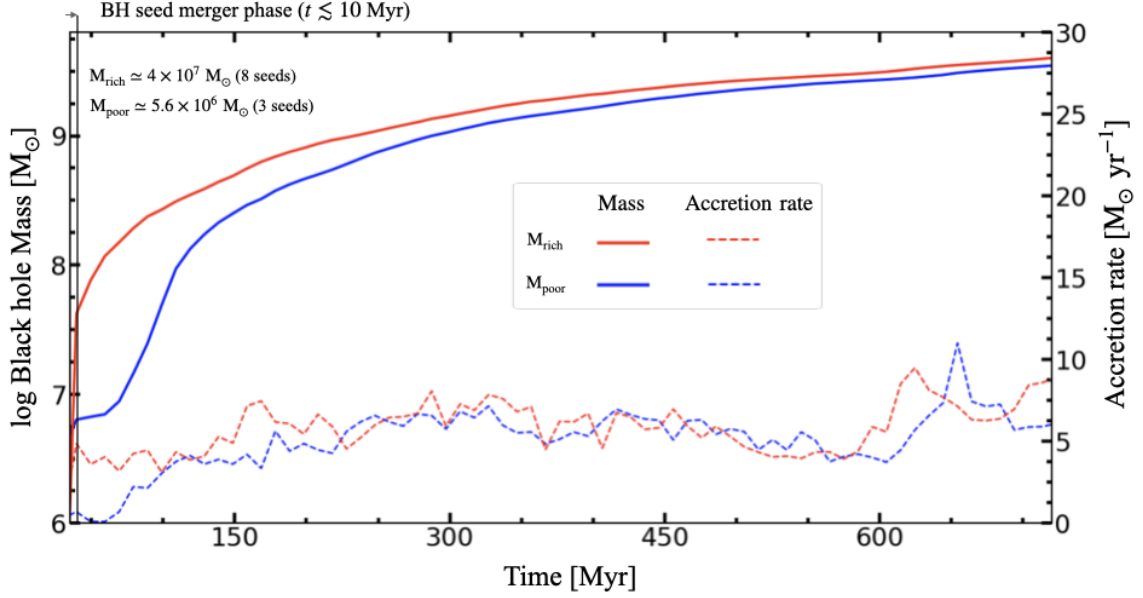


Figure 1. The evolution of SMBHs in the M_{poor} and M_{rich} models. In the M_{poor} model, three BH seeds merge into an SMBH seed with a mass of $5.6 \times 10^6 M_\odot$, while in the M_{rich} model, eight BH seeds merge into an SMBH seed with a mass of $4 \times 10^7 M_\odot$. The average accretion rate is $5 M_\odot \text{ yr}^{-1}$ for the M_{poor} model and $7 M_\odot \text{ yr}^{-1}$ for the M_{rich} model. The SMBH feedback-accretion interaction leads to an oscillatory pattern in the accretion rates.

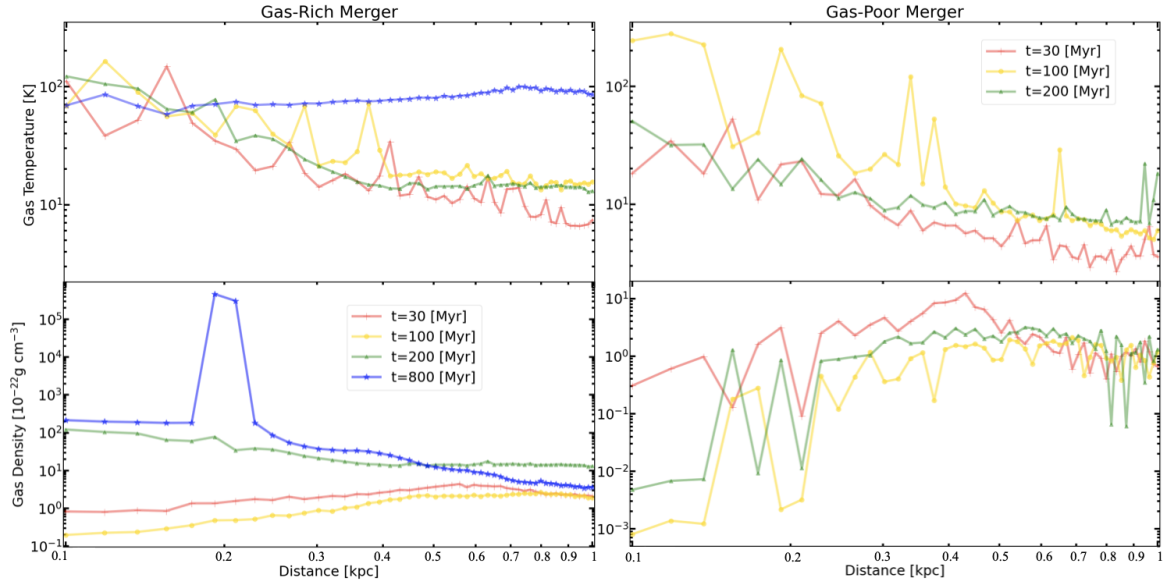


Figure 2. 1D projected gas temperature and density profiles around the SMBH. The red, yellow, green, and blue lines show the radial profiles at $t=30$, 100, 200, and 800 Myr, respectively. We calculate these mass-weighted profiles by projecting the 3D structure of density and temperature into a 1 kpc sphere centered at the SMBH.

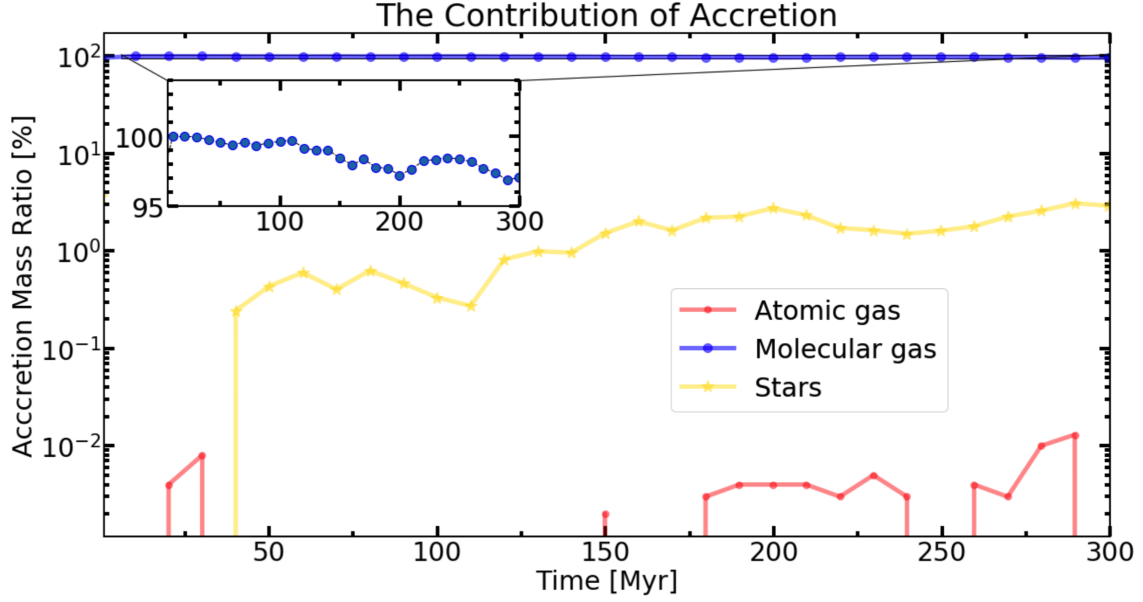


Figure 3. The evolution of accreted compositions is shown by the color curves, representing the accretion of atomic gas, molecular gas, and stars onto the SMBH. It is evident that molecular gas contributes more than 95% of the accretion mass, with the remaining $< 5\%$ coming mostly from stars. The contribution of atomic gas is minimal, accounting for less than 0.01% of the SMBH accretion. Hence, the accretion of molecular gas from giant molecular clouds (GMCs) dominates the mass accretion onto the SMBH.

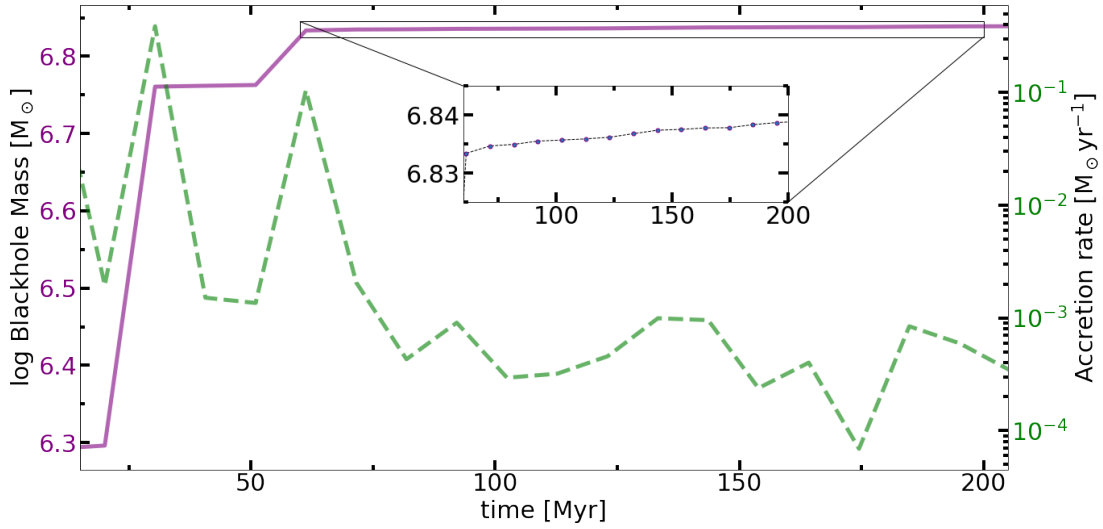


Figure 4. The evolution of SMBH mass in the model with a particle mass of $10^4 M_\odot$ for both molecular and atomic gas. The purple line indicates the SMBH mass evolution, while the green dashed line represents the SMBH mass accretion rate. The initial rapid growth of the BH seed from $2 \times 10^6 M_\odot$ to $5.6 \times 10^6 M_\odot$ in the first 10 Myr is due to the merger of BH seeds discussed in Section 2.4. However, because the molecular gas particle has the same mass as the atomic gas particle, the migration timescale for the “molecular gas particle” toward the galactic center becomes ~ 5 Gyr. Consequently, after 200 Myr, the SMBH only grows to $6.3 \times 10^6 M_\odot$, indicating that inefficient gas accretion fails to drive a rapid SMBH growth.

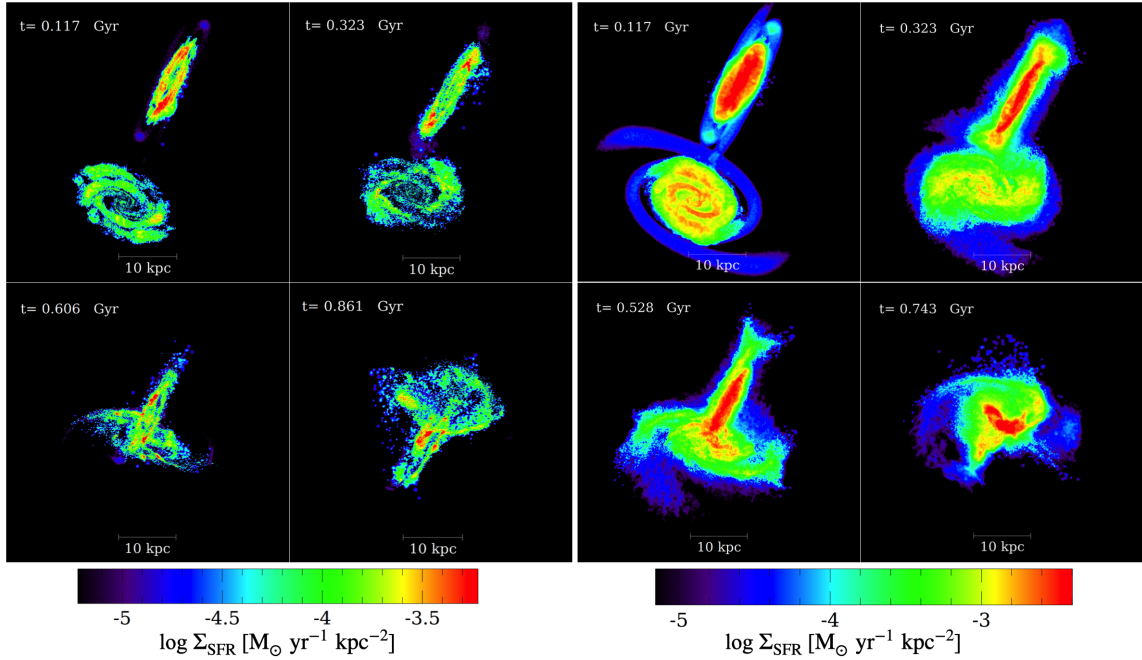


Figure 5. Left: The star formation rate density (Σ_{SFR}) in the model M_{poor} . The strong star formation regions shift from the spiral arms to the centers. Right: The star formation rate density (Σ_{SFR}) in the model M_{rich} . The molecular gas is more concentrated in the central region, and the SFR is enhanced, which drives the nucleus starburst.

newly-acquired dark matter will re-distribute onto the primary galaxy (Ferrarese 2002). Thus, minor mergers can grow the bulge of the primary galaxy in mass and size without destroying the spiral structure.

4. DISCUSSIONS

4.1. Physics and caveat of the SMBH growth

Our results show that the SMBH in the main disk galaxy ($\sim 10^{12} M_{\odot}$) can accrete GMCs to increase its mass via a major merger. This process allows the SMBHs' mass to increase from $10^7 M_{\odot}$ to $10^9 M_{\odot}$ within 300 Myr. Furthermore, the SMBHs in a gas-rich galaxy merger can attain larger masses than those in a gas-poor galaxy merger (Figure 1); this result well matches the results of Di Matteo et al. (2005), but our SMBHs' growth time is considerably shorter than that of Di Matteo et al. (2005).

We discuss the physics and uncertainties associated with our findings, indicating that an SMBH can experience rapid growth by accreting molecular gas. Based on (Chandrasekhar 1943; Carroll & Ostlie 2017; Di Matteo et al. 2019), the dynamical friction in a galaxy can be expressed as:

$$f \simeq 4\pi G^2 C \frac{M^2 \rho}{v_M^2}, \quad (3)$$

where M : the object's mass, v_M : the object's velocity, ρ : the density of the surrounding medium, and C is a function that depends on how v_M compares with

the velocity dispersion of the surrounding medium. The dynamical friction is proportional to the mass squared of the object, as indicated by Equation (3). Because a GMC particle is about 100 times heavier than an atomic gas in the simulation, the dynamical friction for a GMC then becomes 10,000 stronger than atomic gas. Therefore, this strong force will drag the innermost molecular gas toward the galactic center and fuel the growth of an SMBH during major mergers.

Jefferson & Kruijssen (2018) suggest the lifespan of a GMC of $\sim 10 - 100$ Myr that sets an upper limit in the migration time for a bulge GMC moving toward an SMBH. Based on Equation (3), we estimate the migration timescale t_m for a GMC moving from the stellar bulge to the galactic center;

$$\frac{dv_M}{dt_m} \simeq 4\pi G^2 C \frac{M\rho}{v_M^2} \Rightarrow t_m \simeq \frac{v_M^3}{12\pi G^2 C M \rho}, \quad (4)$$

where G : the gravitational constant, M : the GMC's mass $\sim 10^6 M_{\odot}$, v_M : the GMC's drift velocity relative the galactic center, ρ : the matter density of the stellar bulge, and C is ~ 100 for a typical stellar bulge. The matter density is $\rho = 3M_b/4\pi R_b^3$ by assuming a spherical symmetry bulge of mass $M_b \sim 10^{10} M_{\odot}$ with a radius of $R_b \sim 1$ kpc. The drift velocity of a GMC toward the galactic center takes its initial keplerian velocity $v_M \sim \sqrt{GM_b/R_b}$. Equation (4) can be rewritten

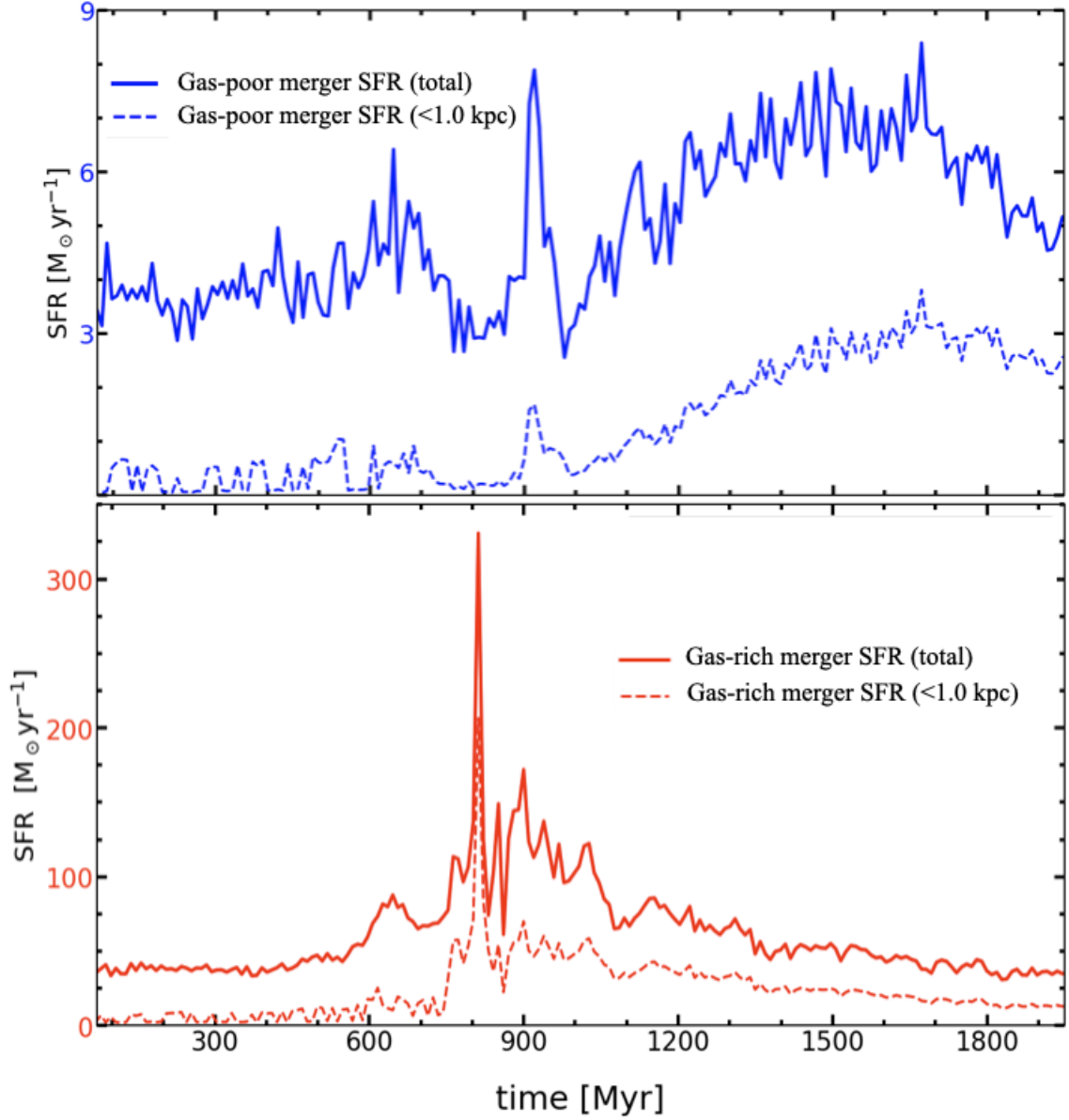


Figure 6. The SFR history during major mergers. In M_{rich} , the SFR reaches $\geq 100 M_{\odot} \text{ yr}^{-1}$ at $t \sim 800$ Myr and lasts for ~ 150 Myr. Such a violent SF event is known as the starburst phenomenon. The dashed lines represent the SFR in the central 1kpc region of the M_{poor} and M_{rich} models, respectively. The trend of the nucleus star formation is highly related to the starburst, implying that a large amount of molecular gas moves to the galactic center during this period.

and yields t_m :

$$t_m \simeq \frac{1}{9C} \frac{M_b}{M} \sqrt{\frac{R_b^3}{GM_b}} \simeq 5 \times 10^7 \text{ yr} \sim 50 \text{ Myr}, \quad (5)$$

which is within the maximum lifespan of a GMC of ~ 100 Myr. Therefore, GMCs can possibly arrive at the galactic center and feed an SMBH before they are dissipated. Some short-lived GMCs of lifespan < 50 Myr may dissipate before accreting onto the SMBH. However, these dissipated clouds may be reformed to GMCs around the galactic center ($R \sim 0.2$ kpc) (Morris

& Serabyn 1996; Genzel et al. 2010; Kauffmann et al. 2017). Furthermore, the successful rapid growth of an SMBH only requires accreting a fraction of halo gas rather than the entire gas from the host galaxy; our assumption of GMCs remains effective in demonstrating the phenomenon that GMCs migrate to the galactic center during galaxy mergers. In comparison, the migration timescale of the atomic-gas particle ($\sim 10^4 M_{\odot}$) is 5000 Myr, which hinders the accretion of atomic gas.

We argue that the massive GMCs have strong dynamical friction for efficient accretion onto an SMBH. How-

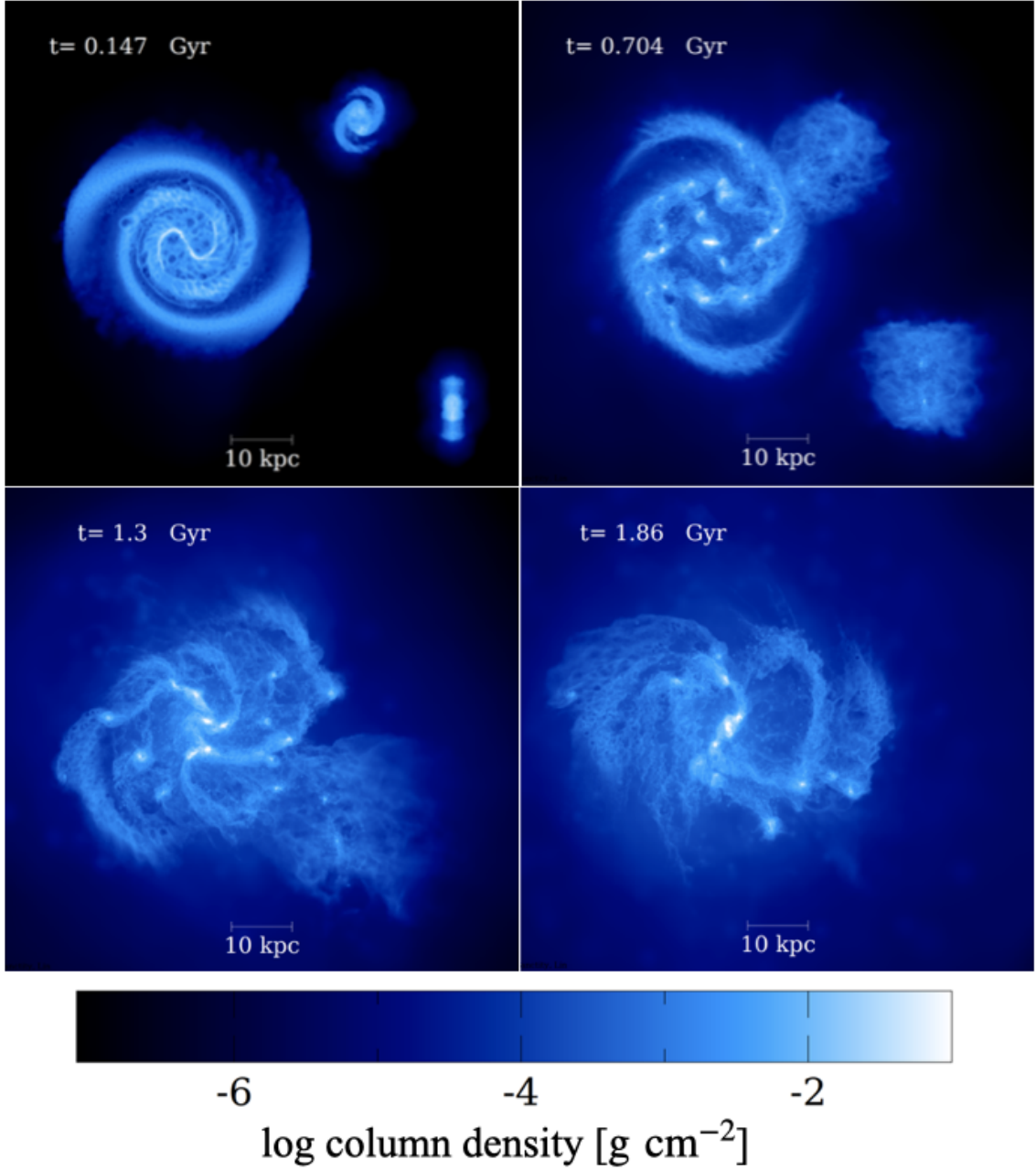


Figure 7. The evolution of minor mergers. The primary galaxy is a gas-poor galaxy, and we put two dwarf galaxies with different tilting angles to the galactic plane placed near the primary galaxy (see Table 2 for the angle information). Unlike the major mergers that disrupt the original spiral arms of the galaxy, minor mergers retain the original spiral arms of the primary galaxy.

ever, each star particle has a mass of $\sim 10^6 M_\odot$, and each dark matter particle has a mass of $\sim 5 \times 10^6 M_\odot$; both also feel strong dynamical friction to drag them into the galactic center. Do star and dark matter particles contribute to the rapid growth of SMBH, too? The star particles have strong stellar feedback, which heats their surrounding environments and alters the mass distribution of gas. As a result, star particles' trajectories

can be disturbed, which prevents these star particles from being swallowed by the SMBH. As for the dark matter accretion, the nature of dark matter is still unknown; whether their particle-like or wave-like behaviors can significantly affect their accretion physics, which is beyond the scope of this study. Therefore, we prohibit the accretion of dark matter onto the SMBHs in the simulation.

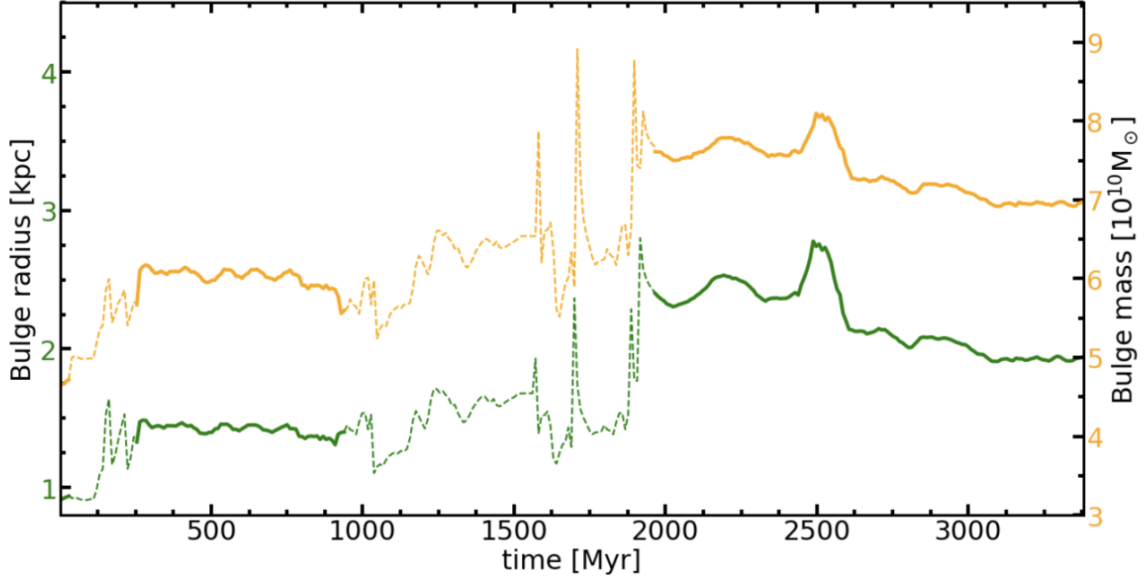


Figure 8. The bulge evolution in the M_{poor} model. The green line represents the bulge size. The initial size of the bulge in the M_{poor} model is 0.92 kpc, and it grows to 1.9 kpc after two minor mergers. The orange line denotes the total mass of the bulge. The initial mass of bulge in the M_{poor} model is $\sim 4.7 \times 10^{10} M_{\odot}$, and it increases to $\sim 7.0 \times 10^{10} M_{\odot}$ after minor mergers. The solid line sections from the bulge fitting refer to the SMBH as the bulge center. However, during minor mergers, the stellar density profile cannot fit well with the sersic function referring to the SMBH. Therefore, we select the position of highest Σ_{*} as the bulge center for fitting, and it yields the dashed line sections.

4.2. Possible destructive and reformation mechanisms of GMCs

Besides the lifetime, several physical processes can destroy GMCs during their journey toward an SMBH. These processes include ram-pressure stripping, tidal disruption, and irradiation. In this section, we will discuss the effects of these mechanisms. To assess the impact of ram-pressure stripping on GMCs, we compare the magnitude of the ram-pressure acting on a GMC (P) to the gravitational binding energy density (U_g). The ram pressure is given by

$$P = \frac{1}{2} \rho v^2 \sim 1.4 \times 10^{-16} \text{ kg} \cdot \text{m}^{-1} \cdot \text{s}^{-2}, \quad (6)$$

where the ISM density, $\rho \sim 1 \text{ particle cm}^{-3} = 1.7 \times 10^{-21} \text{ kg} \cdot \text{m}^{-3}$, and the drift velocity of the molecular cloud toward the galactic center is $v \sim 20/10^5 \text{ pc} \cdot \text{yr}^{-1} = 400 \text{ m} \cdot \text{s}^{-1}$ based on Hsieh et al. (2017). In contrast, the gravitational binding energy density of a GMC

$$U_g \approx \left(\frac{3GM^2}{5R} \right) \frac{3}{4\pi R^3} \sim 4.3 \times 10^{-13} \text{ kg} \cdot \text{m}^{-1} \cdot \text{s}^{-2}, \quad (7)$$

where G is the gravitational constant, M is the GMC mass of $\sim 10^6 M_{\odot} = 2 \times 10^{36} \text{ kg}$ and R is the GMC radius of $\sim 100 \text{ pc} = 3.1 \times 10^{18} \text{ m}$. Because the binding energy of the GMC is about 1000 larger than the ram-pressure from the surrounding medium, the ram-pressure stripping effect of GMCs is neglectable. Irradiation effects are also minimal because dust and H_2 in

GMCs can help to shield from the external UV radiation field. Even if the mechanisms mentioned above disrupt some GMCs, they can be reformed through the compression of diffuse atomic gas in high-pressure environments created by the large-scale shocks from spiral arm passages or stellar feedback from massive stars and supernovae (Clark et al. 2005; Lee et al. 2017). For tidal disruption, a portion of the GMCs debris can be pulled from a distance of 20 pc towards a 2 pc circumnuclear disk (CND) within $\sim 10^5$ years based on the observation of Sagittarius A* (Hsieh et al. 2017). In Seyfert galaxies, star formation can occur in CNDs that supports dense molecular gas to persist in the vicinity of the SMBH, and this CND-scale molecular gas can fuel AGNs (Izumi et al. 2016).

4.3. Relations among SMBH mass, stellar mass, and bulge properties

Reines & Volonteri (2015) found an empirical relation of SMBH mass and stellar mass in S/S0 galaxies with classical bulges and elliptical galaxies,

$$\log\left(\frac{M_{\text{SMBH}}}{M_{\odot}}\right) = (8.95 \pm 0.09) + (1.40 \pm 0.21) \log\left(\frac{M_{*}}{10^{11} M_{\odot}}\right). \quad (8)$$

In the model M_{rich} , the SMBH has a mass of $\sim 10^{10} M_{\odot}$ at $t \sim 2000 \text{ Myr}$. Based on Equation (8), the

corresponding stellar mass is $\sim (6 \pm 4) \times 10^{11} M_{\odot}$. Meanwhile, we obtain the total stellar mass of $1.5 \times 10^{11} M_{\odot}$ by summing up the mass of the existing old stars in the disk and bulge, as well as the mass of newly formed stars from Figure 6. The total stellar mass in M_{rich} falls in the lower end at this empirical relation, yielding an over-massive SMBH compared to the bulge mass. At $t \sim 2000$ Myr, the rapid growth of SMBH is close to the end. However, the violent SF activities are still happening, as shown by the non-decaying SFR in Figure 6. Missing the contribution of unfinished SF drop the total stellar mass to the lower end. Besides, the stellar mass of a galaxy can also increase through minor mergers (see Fig. 8). Because events of gas-rich major mergers are rare, minor and/or gas-poor mergers can replenish the missing stellar mass. In the model M_{poor} , the mass of SMBH is $\sim 3 \times 10^9 M_{\odot}$ with a total stellar mass of $2.6 \times 10^{11} M_{\odot}$ at $t = 2000$ Myr. If we put the $3 \times 10^9 M_{\odot}$ SMBH in Equation (8), the resulting stellar mass would be $(1.8 \pm 1.2) \times 10^{11} M_{\odot}$, which matches well with the result from the M_{poor} model. In the simulation, we observed two kinds of active star formation. During the merger of gas-poor galaxies, their SFR increases by a factor of 2 to 3, which agrees well with the observational results of Pearson et al. (2019) for low-redshift galaxies. However, during the merge of the gas-rich galaxies, their SFR significantly increases and exhibits a nucleus starburst shown in Figure 6. The timescale for the starburst is 150 Myr, which is close to the observational merger samples of 10^7 yr to a few 10^8 yr in Cortijo-Ferrero et al. (2017). The large SFR stems from the merger-driven central star formation (Barnes & Hernquist 1991; Mihos & Hernquist 1995; Saitoh et al. 2009; Sparre & Springel 2016) when the fresh molecular gas flows into the galactic center and forms numerous stars. In comparison, if the original molecular model in GIZMO is used, no starburst is found during both gas-poor and gas-rich mergers. Our results also show that the bulge in a spiral galaxy can be grown through minor mergers (Bédorf & Portegies Zwart 2013). For the minor merge of a gas-poor galaxy, its bulge radius grows from 0.9 kpc to 1.9 kpc, and mass increase from $4.7 \times 10^{10} M_{\odot}$ to $7.0 \times 10^{10} M_{\odot}$ after two minor mergers with dwarf galaxies. Because the Sagittarius A* is only $\sim 10^6 M_{\odot}$, we suspect that our Milky Way may not have undergone any major mergers in its lifetime.

4.4. Limitations of models

Although our molecular gas model can realize the rapid growth of SMBHs, it still has several drawbacks to be improved. The accretion rate depicted in Figure 1 represents an idealized maximum value based on the

assumption of massive GMCs with a mass of $10^6 M_{\odot}$, rather than a more realistic mass distribution ranging from $10^5 M_{\odot} - 10^6 M_{\odot}$ (Rosolowsky 2005; Blitz et al. 2006). Additionally, the assumption of a 100% survival rate for GMCs during migration to the galactic centers is unrealistic, as GMCs can be subject to destructive mechanisms such as tidal disruption, ram-pressure stripping, and irradiation. However, replenishing dissipated GMCs through new molecular cloud formation is also possible. Furthermore, major mergers are rare events. Observations suggest that the number of major mergers is lower than that of active galactic nuclei (AGNs) in the redshift range of $0 < z < 3$ (Treister et al. 2010). Therefore, rapid SMBH growth via major mergers is more likely to occur in the high- z universe, where interactions among galaxies are frequent.

Our simulation cannot model the formation and destruction of molecular gas from the first principles. As the first attempt, we adopt constant ratios of the molecular and atomic/ionized gas in the simulation. The bottleneck is to model the chemistry of multi-phase and multi-component ISM, and simultaneously differentiate the dynamics of molecular cloud and diffuse gas that remains beyond the envelope of our current ISM modeling. Recently, good progress has been made to improve the gas chemistry for galaxy simulations; for example, Popping et al. (2014) developed a molecular hydrogen formation recipes, and Hopkins et al. (2018, 2023) estimated the molecular hydrogen fraction based on the thermo-chemical equilibrium.

5. CONCLUSION

In this study, we have presented the simulations of merging galaxies with GIZMO. Our simulation contains the major mergers of gas-poor and gas-rich galaxies as well as minor mergers. We find that the dynamics of GMCs play an essential role in galaxy mergers. Massive molecular gas particles can more efficiently lose their kinetic energy than atomic-gas particles due to stronger dynamical friction, which causes them to fall into the galaxy's center. Consequently, SMBHs can grow from $10^7 M_{\odot}$ to $10^9 M_{\odot}$ within 300 Myr, providing a possible explanation for the creation of massive SMBH ($10^9 M_{\odot}$) in the early universe.

The SFRs in the galaxy mergers also become higher than those in the isolated case, and $\sim 50\%$ of the star formation occurs in the central region; the SFRs can even reach the starburst phase during a period of wet major merger, where more than 65% of star formation occurs in the center of the galaxy. This result strengthens the idea that the dynamics difference between atomic and molecular gas particles leads to the merger-driven star-

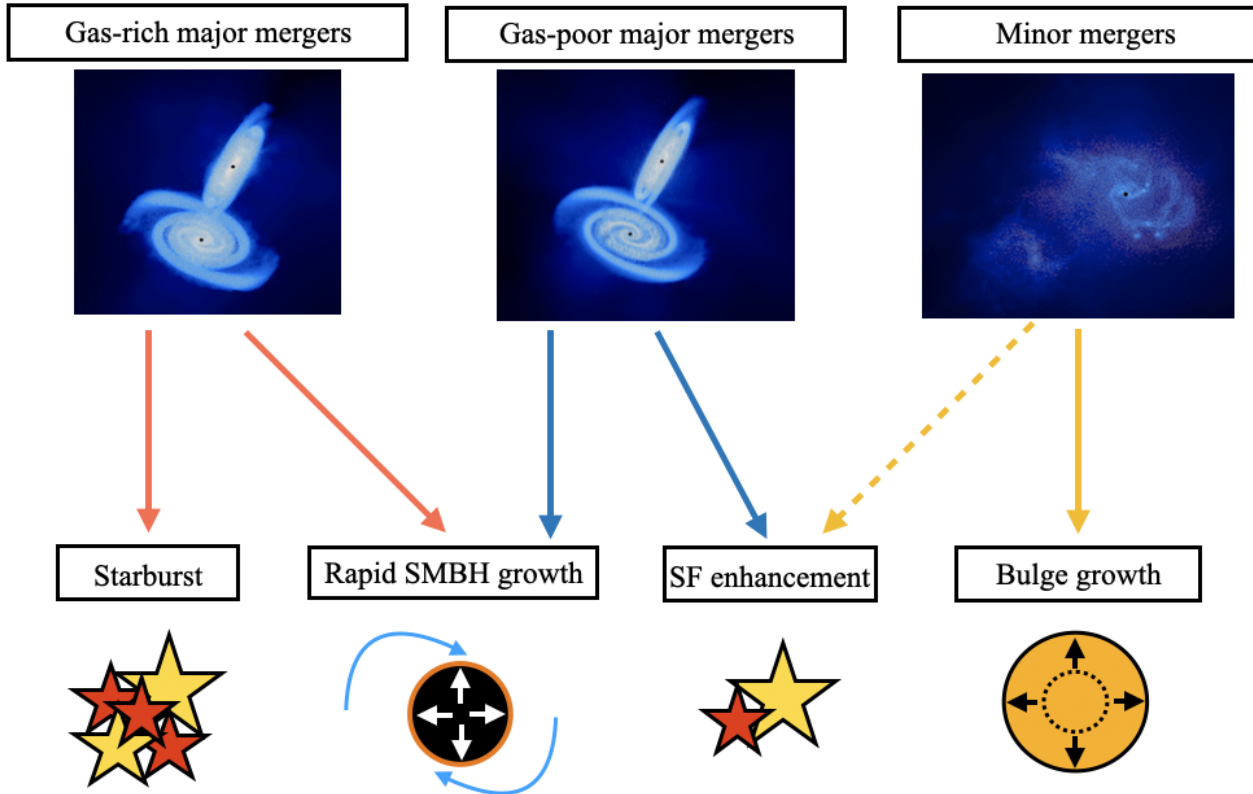


Figure 9. This schematic illustrates the consequences of galaxy mergers. The red line represents the major merger of a gas-rich disk galaxy, the blue line represents the major merger of a gas-poor galaxy, and the yellow line represents the minor merger of a gas-poor galaxy. The solid lines represent the outcomes of the simulation, while the dashed lines depict possible evolution tracks. Following the rapid growth of the SMBH, its mass reaches a threshold level that triggers strong feedback, leading to gas ejection from the host galaxy.

burst. Similarly, in the merger of gas-poor galaxies, the SFR can be increased by a factor of 2 to 3 in the galactic center area. Furthermore, we can grow the bulge of a gas-poor disk galaxy through minor mergers, and the size and mass of the bulge can increase from 0.92 kpc to 1.9 kpc and from $4.7 \times 10^{10} M_{\odot}$ to $7 \times 10^{10} M_{\odot}$, respectively. A galaxy with a prominent bulge is likely to experience many minor mergers during its evolution. Based on the simulation, we suggest that the Milky Way has experienced many minor mergers but no major mergers. We summarize the scenarios of galaxy mergers based on the simulation in Figure 9.

This study sheds light on the rapid growth of SMBHs and the bulge evolution in interacting galaxies. Combining sophisticated models with the upcoming high-sensitivity surveys by James Webb Space Telescope (*JWST*) and the Vera C. Rubin Observatory (*LSST*), we will be able to unveil the physics behind the growth of SMBHs and their host galaxies in the early universe.

Authors are grateful to the anonymous referee for his/her constructive suggestions that significantly improve the quality of this paper. We also thank Yen-Chen Pan and You-Hua Chu for their valuable comments. S.L. thanks Ching-Yao Tang for his encouragement and discussion. This work was supported by the National Science and Technology Council, Taiwan, under grant no. MOST 110-2112-M-001-068-MY3 and MOST 110-2112-M-008-021-MY3, as well as by the Academia Sinica, Taiwan, under a career development award, grant no. ASCDA-111-M04. Our computational resources are provided by the National Energy Research Scientific Computing Center (NERSC), a U.S. Department of Energy Office of Science User Facility operated under Contract No. DE-AC02-05CH11231, and the TIARA Cluster at the Academia Sinica Institute of Astronomy and Astrophysics (ASIAA).

Acknowledgement

REFERENCES

- Aller, M., & Richstone, D. 2007, *The Astrophysical Journal*, 665, 120
- Barnes, J. E., & Hernquist, L. E. 1991, *The Astrophysical Journal*, 370, L65
- Bédorf, J., & Portegies Zwart, S. 2013, *Monthly Notices of the Royal Astronomical Society*, 431, 767
- Begelman, M. C. 2010, *Monthly Notices of the Royal Astronomical Society*, 402, 673
- Blitz, L., Fukui, Y., Kawamura, A., et al. 2006, arXiv preprint astro-ph/0602600
- Borguet, B. C., Arav, N., Edmonds, D., Chamberlain, C., & Benn, C. 2012, *The Astrophysical Journal*, 762, 49
- Bournaud, F., Jog, C., & Combes, F. 2005, *Astronomy & Astrophysics*, 437, 69
- Brown, A. G., Vallenari, A., Prusti, T., et al. 2016, *Astronomy & Astrophysics*, 595, A2
- Carroll, B. W., & Ostlie, D. A. 2017, *An introduction to modern astrophysics* (Cambridge University Press)
- Chabrier, G. 2003, *The Astrophysical Journal*, 586, L133
- Chandrasekhar, S. 1943, *Astrophysical Journal*, 97, 255
- Chen, K.-J., Heger, A., Woosley, S., et al. 2014, *The Astrophysical Journal*, 790, 162
- Clark, P. C., Bonnell, I. A., Zinnecker, H., & Bate, M. R. 2005, *Monthly Notices of the Royal Astronomical Society*, 359, 809
- Cohen, R., Grabelsky, D., May, J., et al. 1985, *The Astrophysical Journal*, 290, L15
- Collette, A. 2013, *Python and HDF5: unlocking scientific data* ("O'Reilly Media, Inc.")
- Cortijo-Ferrero, C., Delgado, R. G., Pérez, E., et al. 2017, *Astronomy & Astrophysics*, 607, A70
- Das, A., Schleicher, D. R., Leigh, N. W., & Boekholt, T. C. 2021, *Monthly Notices of the Royal Astronomical Society*, 503, 1051
- Di Matteo, T., King, A., & Cornish, N. J. 2019, *Black hole formation and growth* (Springer)
- Di Matteo, T., Springel, V., & Hernquist, L. 2005, *nature*, 433, 604
- Eliche-Moral, M. C., González-García, A. C., Balcels, M., et al. 2011, *Astronomy & Astrophysics*, 533, A104
- Faucher-Giguère, C.-A. 2020, *Monthly Notices of the Royal Astronomical Society*, 493, 1614
- Feoli, A., Mancini, L., Marulli, F., & van den Bergh, S. 2011, *General Relativity and Gravitation*, 43, 1007
- Ferland, G., Korista, K., Verner, D., et al. 1998, *Publications of the Astronomical Society of the Pacific*, 110, 761
- Ferrarese, L. 2002, *The Astrophysical Journal*, 578, 90
- Ferrarese, L., & Merritt, D. 2000, *The Astrophysical Journal Letters*, 539, L9
- Fujii, M. S., Bédorf, J., Baba, J., & Portegies Zwart, S. 2019, *Monthly Notices of the Royal Astronomical Society*, 482, 1983
- Genzel, R., Eisenhauer, F., & Gillessen, S. 2010, *Reviews of Modern Physics*, 82, 3121
- Ghez, A. M., Salim, S., Weinberg, N., et al. 2008, *The Astrophysical Journal*, 689, 1044
- Graham, A. W., & Driver, S. P. 2007, *The Astrophysical Journal*, 655, 77
- Graham, A. W., Erwin, P., Caon, N., & Trujillo, I. 2001, *The Astrophysical Journal Letters*, 563, L11
- Grudić, M. Y., Hopkins, P. F., Faucher-Giguère, C.-A., et al. 2018, *Monthly Notices of the Royal Astronomical Society*, 475, 3511
- Häring, N., & Rix, H.-W. 2004, *The Astrophysical Journal Letters*, 604, L89
- Hopkins, P. F. 2015, *Monthly Notices of the Royal Astronomical Society*, 450, 53
- Hopkins, P. F., Hernquist, L., Cox, T. J., et al. 2006, *The Astrophysical Journal Supplement Series*, 163, 1
- Hopkins, P. F., & Quataert, E. 2010, *Monthly Notices of the Royal Astronomical Society*, 407, 1529
- . 2011, *Monthly Notices of the Royal Astronomical Society*, 415, 1027
- Hopkins, P. F., Torrey, P., Faucher-Giguère, C.-A., Quataert, E., & Murray, N. 2016, *Monthly Notices of the Royal Astronomical Society*, 458, 816
- Hopkins, P. F., Bundy, K., Croton, D., et al. 2010, *The Astrophysical Journal*, 715, 202
- Hopkins, P. F., Wetzel, A., Kereš, D., et al. 2018, *Monthly Notices of the Royal Astronomical Society*, 480, 800
- Hopkins, P. F., Wetzel, A., Wheeler, C., et al. 2023, *Monthly Notices of the Royal Astronomical Society*, 519, 3154
- Hoyle, F., & Fowler, W. A. 1962, *Monthly Notices of the Royal Astronomical Society*, 125, 169
- Hsieh, P.-Y., Koch, P. M., Ho, P. T., et al. 2017, *The Astrophysical Journal*, 847, 3
- Hunter, J. D. 2007, *IEEE Annals of the History of Computing*, 9, 90
- Inayoshi, K., Visbal, E., & Haiman, Z. 2020, *Annual Review of Astronomy and Astrophysics*, 58, 27
- Izumi, T., Kawakatu, N., & Kohno, K. 2016, *The Astrophysical Journal*, 827, 81
- Jeffreson, S. M., & Kruijssen, J. D. 2018, *Monthly Notices of the Royal Astronomical Society*, 476, 3688

- Joseph, R., & Wright, G. 1985, *Monthly Notices of the Royal Astronomical Society*, 214, 87
- Kauffmann, J., Pillai, T., Zhang, Q., et al. 2017, *Astronomy & Astrophysics*, 603, A89
- Kim, J.-h., Agertz, O., Teyssier, R., et al. 2016, *The Astrophysical Journal*, 833, 202
- King, A., & Pounds, K. 2015, *Annual Review of Astronomy and Astrophysics*, 53, 115
- Kormendy, J., & Ho, L. C. 2013, *Annual Review of Astronomy and Astrophysics*, 51, 511
- Kormendy, J., & Richstone, D. 1995, *Annual Review of Astronomy and Astrophysics*, 33, 581
- Lamberts, A., Garrison-Kimmel, S., Clausen, D., & Hopkins, P. 2016, *Monthly Notices of the Royal Astronomical Society: Letters*, 463, L31
- Lauer, T. R., Faber, S., Richstone, D., et al. 2007, *The Astrophysical Journal*, 662, 808
- Lee, B., Chung, A., Tonnesen, S., et al. 2017, *Monthly Notices of the Royal Astronomical Society*, 466, 1382
- Li, E. 2016, arXiv preprint arXiv:1612.07781
- Lynden-Bell, D. 1969, *Nature*, 223, 690
- Magorrian, J., Tremaine, S., Richstone, D., et al. 1998, *The Astronomical Journal*, 115, 2285
- Marconi, A., & Hunt, L. K. 2003, *The Astrophysical Journal Letters*, 589, L21
- Marinacci, F., Sales, L. V., Vogelsberger, M., Torrey, P., & Springel, V. 2019, *Monthly Notices of the Royal Astronomical Society*, 489, 4233
- McKee, C. F., & Ostriker, J. P. 1977, *The Astrophysical Journal*, 218, 148
- McLure, R., & Dunlop, J. 2002, *Monthly Notices of the Royal Astronomical Society*, 331, 795
- Mihos, C., & Hernquist, L. 1995, arXiv preprint astro-ph/9512099
- Moe, M., Arav, N., Bautista, M. A., & Korista, K. T. 2009, *The Astrophysical Journal*, 706, 525
- Morris, M., & Serabyn, E. 1996, *Annual Review of Astronomy and Astrophysics*, 34, 645
- Mortlock, D. J., Warren, S. J., Venemans, B. P., et al. 2011, *Nature*, 474, 616
- Pearson, W., Wang, L., Alpaslan, M., et al. 2019, *Astronomy & Astrophysics*, 631, A51
- Perret, V., Renaud, F., Epinat, B., et al. 2014, *Astronomy & Astrophysics*, 562, A1
- Popping, G., Somerville, R. S., & Trager, S. C. 2014, *Monthly Notices of the Royal Astronomical Society*, 442, 2398
- Posti, L., & Helmi, A. 2019, *Astronomy & Astrophysics*, 621, A56
- Price, D. J. 2007, *Publications of the Astronomical Society of Australia*, 24, 159
- Quataert, E., Narayan, R., & Reid, M. J. 1999, *The Astrophysical Journal Letters*, 517, L101
- Rees, M. J. 1984, *Annual review of astronomy and astrophysics*, 22, 471
- Reines, A. E., & Volonteri, M. 2015, *The Astrophysical Journal*, 813, 82
- Robertson, B. E., & Kravtsov, A. V. 2008, *The Astrophysical Journal*, 680, 1083
- Rosolowsky, E. 2005, *Publications of the Astronomical Society of the Pacific*, 117, 1403
- Rozwadowska, K., Vissani, F., & Cappellaro, E. 2021, *New Astronomy*, 83, 101498
- Saitoh, T. R., Daisaka, H., Kokubo, E., et al. 2009, *Publications of the Astronomical Society of Japan*, 61, 481
- Schweizer, F. 2005, in *Starbursts* (Springer), 143–152
- Sersic, J. L. 1968, *Cordoba*
- Shakura, N. I., & Sunyaev, R. A. 1973, *Astronomy and Astrophysics*, 24, 337
- Soker, N., & Meiron, Y. 2011, *Monthly Notices of the Royal Astronomical Society*, 411, 1803
- Solomon, P., Rivolo, A., Barrett, J., & Yahil, A. 1987, *The Astrophysical Journal*, 319, 730
- Solomon, P., Sanders, D., & Scoville, N. 1979, in *Symposium-International Astronomical Union, Vol. 84*, Cambridge University Press, 35–52
- Solomon, P., & Vanden Bout, P. 2005, *Annu. Rev. Astron. Astrophys.*, 43, 677
- Solomon, P. M., & Sanders, D. 1980, in *Giant Molecular Clouds in the Galaxy* (Elsevier), 41–73
- Sparre, M., & Springel, V. 2016, *Monthly Notices of the Royal Astronomical Society*, 462, 2418
- Springel, V. 2005, *Monthly notices of the royal astronomical society*, 364, 1105
- Springel, V., Di Matteo, T., & Hernquist, L. 2005a, *The Astrophysical Journal*, 620, L79
- . 2005b, *Monthly Notices of the Royal Astronomical Society*, 361, 776
- Springel, V., & Hernquist, L. 2003, *Monthly Notices of the Royal Astronomical Society*, 339, 289
- Takeo, E., Inayoshi, K., Ohsuga, K., Takahashi, H. R., & Mineshige, S. 2019, *Monthly Notices of the Royal Astronomical Society*, 488, 2689
- Treister, E., Natarajan, P., Sanders, D. B., et al. 2010, *Science*, 328, 600
- Tremaine, S., Gebhardt, K., Bender, R., et al. 2002, *The Astrophysical Journal*, 574, 740

- Venemans, B., Bañados, E., Decarli, R., et al. 2015, The Astrophysical Journal Letters, 801, L11
- Virtanen, P., Gommers, R., Oliphant, T. E., et al. 2020, Nature methods, 17, 261
- Vogelsberger, M., Genel, S., Sijacki, D., et al. 2013, Monthly Notices of the Royal Astronomical Society, 436, 3031
- Volonteri, M., & Rees, M. J. 2005, The Astrophysical Journal, 633, 624
- Wandel, A. 2002, The Astrophysical Journal, 565, 762
- Wiersma, R. P., Schaye, J., & Smith, B. D. 2009, Monthly Notices of the Royal Astronomical Society, 393, 99
- Woods, T. E., Agarwal, B., Bromm, V., et al. 2019, Publications of the Astronomical Society of Australia, 36
- Wu, X.-B., & Han, J. 2001, Astronomy & Astrophysics, 380, 31